Environmental Science
Processes & Impacts

Use of optical properties for evaluating the presence of pyrogenic organic matter in thermally altered soil leachates

Journal:	*Environmental Science: Processes & Impacts*
Manuscript ID	EM-ART-09-2019-000413.R2
Article Type:	Paper

Use of optical properties for evaluating the presence of pyrogenic organic matter in thermally altered soil leachates

Garrett McKay,[1*] Amanda K. Hohner,[2*] and Fernando L. Rosario-Ortiz[3]

[1]Zachry Department of Civil and Environmental Engineering, Texas A&M University, College Station, TX; [2]Department of Civil and Environmental Engineering, Washington State University, Pullman, WA; [3]Department of Civil, Environmental, and Architectural Engineering, University of Colorado Boulder, Boulder, CO

*Corresponding authors: gmckay@tamu.edu; ahohner@wsu.edu
Submitted to *Environmental Science: Processes and Impacts*

Abstract

The increased frequency and severity of wildfires in forested watersheds has the potential to significantly impact the quantity and quality of water extractable organic matter (WEOM) exported from these ecosystems. This study examined the optical properties of WEOM from laboratory heated soil in order to understand physicochemical changes occurring in the organic matter as a result of heating, as well as test the usefulness of optical parameters for assessing the presence of pyrogenic organic matter. WEOM absorbance and fluorescence spectral shape and intensity varied systematically as a function of soil heating temperature. Notably, absorbance and fluorescence intensity, specific ultraviolet absorbance, apparent fluorescence quantum yield, specific fluorescence emission intensity, and maximum fluorescence emission wavelength exhibited consistent changes with heating temperature and indicated that WEOM in heated soil leachates was lower in molecular weight and more aromatic than in unheated samples. The lower molecular weight in heated soil WEOM was corroborated with size-exclusion chromatography measurements. This work increases the understanding of the molecular changes occurring in WEOM as a result of wildfire and indicates that optical measurements (i.e., absorbance and fluorescence) could be used for watershed monitoring of post-fire pyrogenic organic matter.

Environmental Significance

Wildfires have significant potential to influence the amount and character of water extractable organic matter (WEOM) exported from forested watersheds. This study uses absorbance and fluorescence spectroscopy to examine the effect of laboratory heating of soils on WEOM physicochemical properties. The systematic changes in optical properties observed provide insight into molecular changes in WEOM occurring as a result of soil heating and indicate the possibility of using optical measurements for assessing the presence of pyrogenic organic matter post-fire.

Introduction

Wildfire activity and severity has increased in many regions globally, and current projections indicate a continued rise in wildfires as a result of climate change, increased fuel loads, and human activity in the wildland-urban-interface.[1-4] Although wildfires are natural events, they can dramatically alter forest ecosystems and influence the biogeochemical processes that control water quality. As a consequence, wildfires can have short and long-term impacts on forest watersheds that provide critical ecosystem services and drinking water supplies to downstream communities.[5-7]

The complex effects of wildfire on water quality vary due to wildfire behavior, severity, and extent,[8] as well as watershed characteristics.[9,10] Further, precipitation events can enhance the mobilization of ash, soil, nutrients, and organic matter to surface waters, and alter water quality.[11,12] An observed increase in streamwater particulate levels, nutrients, metals, and organic carbon have been reported following wildfires.[5,6] Combustion completeness and the production of pyrogenic material, among many additional wildfire, forest catchment, and hydrologic factors that influence post-fire effects make predicting any single water quality response extremely challenging.

A significant concern following wildfire events is not only that concentrations and loads of exported WEOM will change, but also that the quality and thus the reactivity and fate of this WEOM will change. Changes in WEOM can influence drinking water treatment process performance (e.g., coagulation, disinfection byproduct formation) and environmental processes (e.g., metal transport, aquatic photochemistry). Recent studies have sought to understand the effects of wildfire on WEOM characteristics.[12-15] Wang et al. observed systematic changes in absorbance and fluorescence spectral intensity and

shape, and also chlorine reactivity in WEOM from field-collected ash and laboratory heated material. [13,14] A study by Cawley et al. reported similar results for heated soils and also examined the molecular composition of WEOM by ultra high resolution mass spectrometry, noting that heating resulted in increased amounts of black carbon and black nitrogen formulas in WEOM.[15] In addition, a field study of the Cache la Poudre watershed in Colorado, USA following a wildfire in 2013 demonstrated differences in water quality parameters and disinfection byproduct precursor reactivity between unburned and wildfire-impacted areas of the watershed.[12] Taken as a whole, these studies suggest that changes in WEOM quality due to soil heating have the potential to influence both natural and engineered systems that may be impacted by wildfires.

Despite this previous work, there is still a need to better understand the molecular changes occurring in WEOM as a result of soil heating. Furthermore, it would be beneficial, both from a natural systems and engineering perspective, to be able to track the presence of pyrogenic organic matter in aquatic environments affected by wildfire events. The purpose of this study was to evaluate changes in WEOM optical properties following laboratory heating of soils. To this end, mineral and organic soil layers collected from the Boulder Creek Watershed, Colorado, USA were heated between 100 and 550 ºC in 100 ºC increments to assess the effect of low, moderate, and high heating temperatures. The heated soils were leached into ultra-pure water and WEOM was characterized. Results from additional soils collected from other locations in the USA were consistent with the results obtained for the two locations in Colorado. This work improves the understanding of the effect of wildfire on organic matter optical properties and demonstrates their potential for monitoring post-fire source water quality changes.

Materials and Methods

Soil collection and processing

Soil was collected from the mineral (A horizon) and organic (O horizon) layers at two locations in the Boulder Creek Watershed, Colorado, USA. The first site was north of Nederland, CO (39˚58'52"N 105˚31'07"W, referred to as NED). The NED site had no closed canopy with understory vegetation characterized by blue grama grass (*Bouteloua gracilis)*, needle-and-thread grass (*Hesperostipa comate*), and western wheatgrass (*Pascopyrum smithii*). The NED soil series is moderately permeable and well-drained, characterized by a cobbly sandy loam. The second site was collected from Flagstaff Mountain, Boulder, CO (39˚59'51"N 105˚18'33"W, referred to as FLG). The FLG site samples were taken under closed canopy, which was characterized by coniferous forest stands comprised of ponderosa pine, Douglas fir, and subalpine fir-Engelmann spruce (*Picea engelmanni, Abies lasiocarpa*). There was no prominent understory vegetation; however, a layer of fallen litter consisting chiefly of pine needles was present and was removed prior to mineral soil excavation. Organic soil collected represented the uppermost layer of organic debris on the ground, including some vegetation.

Soil samples were processed immediately after sampling. Mineral soils were distributed on metal trays to a depth of approximately 1 cm and oven-dried at 100˚C for two hours to eliminate moisture and to suppress the survival of microbial communities present in the soil. Mineral soil was then passed through both a 2 mm (No. 10) stainless steel sieve to remove large rocks and plant matter and through a 0.841 mm (No. 20) sieve to remove smaller plant matter before storage. Organic soils were processed similarly to mineral soils (besides sieving).

Mineral soils were heated to temperatures of 150, 250, 350, 450, and 550 ºC in 90-mL porcelain dish crucibles using an electric muffle furnace (Lindberg/Blue Box, Model BF51442C with a Lindberg Furnace Power Supply Controller Model 59344). Organic soils were heated to temperatures of 150, 250, 350, and 450 ºC in loaf pans. Results for 550 ºC were excluded due to limited sample volume, as organic soil heated to this temperature had significant mass loss and anticipated negligible levels of carbon and nitrogen. Soils dried at 100 ºC were considered the control (CTRL) samples. For this study, CTRL/150 ºC, 250/350ºC, and 450/550ºC were considered to encompass unburned/low, moderate, and high heating, respectively. Additional details regarding use of the muffle furnace are provided in ESI Text S1.

Samples were held at each temperature in oxic conditions for 2 hours and once cooled, stored in either amber glass 40 mL vials or half-pint glass jars at room temperature. To ensure uniformity in mineral soil heating, 10 g soil per crucible (approximately 0.5 cm high) was heated in batches of 10 crucibles. Intact organic soil was loosely placed in the loaf pans to ensure uniform heating. After heating, organic soils were mechanically ground using an 8150 Enclosed Shatterbox for 15 seconds, producing a fine powder, and then immediately stored in sterilized mason jars.

Heated soils were leached in ultra-pure water (resistivity = 18.2 MΩ•cm). Mineral and organic soils were added at 5 g L^{-1} and 0.2 g L^{-1} (in a 1 L volume), respectively, and leached for a duration of 6 hr on a shaker table. All leachates were passed through pre-rinsed 0.5 µm disc filters (EMD Millipore Express PLUS Membrane). Leachates were stored at 4 ºC in 1 L glass amber bottles. Additional details related to sample collection, location, and heating temperature are provided in the ESI Table S1.

Analytical methods

The filtered samples were analyzed for dissolved organic carbon (DOC), dissolved organic nitrogen (DON), C and N content, optical properties (absorbance and fluorescence), nitrate/nitrite, and metal content. DOC concentrations were measured with a Shimadzu TOC-V CSN Total Organic Carbon Analyzer with a total nitrogen (TN) unit in replicates of four. Dissolved organic nitrogen (DON) was measured by subtracting dissolved inorganic nitrogen (DIN) from TDN. Nitrite, nitrate, and ammonium were measured at the Arikaree Environmental Laboratory in the Institute for Arctic and Alpine Research at CU Boulder. Nitrite and nitrate were measured using a Lachat QuickChem 8500 Flow Injection Module. Ammonium was measured using a BioTek Synergy 2 Multi-Detection Microplate Reader. The DIN species were measured in replicates of four. C and N fractions in soil were measured in duplicate using a Thermo Scientific Flash EA1112 Nitrogen and Carbon Analyzer. The water extractable organic carbon and organic nitrogen (WEOC and WEON) were calculated from the DOC or DON leached per unit total soil C and N, respectively, remaining after heating. Metals were measured using ICP-OES by the Laboratory for Geological Sciences at CU Boulder.

Absorbance spectra were measured in 1, 5 or 10 cm quartz cuvettes with a Cary-100 Bio UV-Vis spectrophotometer. Fluorescence spectra were measured with a Fluoromax-4 spectrofluorometer in duplicate from 300 nm to 700 nm in 2 nm increments from excitation wavelengths of 240 nm to 550 nm collected in 10 nm increments. The emission detector was set to an integration time of 0.1 s and the excitation and emission bandpass was set to 5 nm. Spectra were blank subtracted, corrected for inner filter effects, had Rayleigh scatter excised, and normalized to Raman area. Raman area was measured daily at an excitation

wavelength of 350 nm with identical instrument settings used for sample collection. It was necessary to dilute several samples with ultra-pure water prior to fluorescence analysis in order to not exceed the linear working range of the emission detector (2×10^6 counts per second). In addition, instrument-specific correction factors were applied to all fluorescence data. Absorbance spectra required for inner filter corrections and fluorescence quantum yield calculations were corrected by the dilution factor used for fluorescence spectra acquisition. No attempt was made to adjust for sample pH as a result of these dilutions; these values are expected to be within pH 6-8.

Size Exclusion Chromatography (SEC) was employed to assess the molecular weight distribution of WEOM. An Agilent 1100 high pressure liquid chromatograph equipped with a protein-pak column (Waters) and UV detector (monitored at 254 nm) was used. The mobile phase consisted of a 10 mM phosphate buffer solution (pH 6.8) and 0.5 M sodium sulfate at a flow rate of 0.7 mL min^{-1}. Sample conductivity was matched to the eluent prior to sample injection. Larger molecular weight compounds elute at earlier times in SEC. Lower molecular weight compounds have more interactions in the pores of the packing material, resulting in longer retention times.

Calculation of optical properties

Optical properties were calculated from absorbance and fluorescence spectra using previously described methods. *E2/E3*, spectral slope ($S_{300\text{-}600}$), and the spectral slope ratio (S_R) were calculated from absorbance spectra. The *E2/E3* ratio represents the ratio of absorbance values at 250 nm and 365 nm. [16] $S_{300\text{-}600}$ (units of nm^{-1}) is derived from non-linear regression analysis of absorbance data between 300 nm and 600 nm to $A(\lambda) = A(350\ \mathrm{nm}) \times \exp\left(-S_{300-600}(\lambda - 350\mathrm{nm})\right)$.[17] The slope ratio, S_R, is calculated

by the ratio of slopes obtained by linearly regressing log-transformed absorbance versus wavelength for the regions 275 nm to 295 nm and 350 nm to 400 nm. [18] $SUVA_{254}$ (units of L mg_C^{-1} m^{-1}) is calculated as the decadic absorbance at 254 nm divided by DOC.[19] Molar extinction coefficients were calculated on a per molar carbon basis (decadic absorbance divided by mol C L^{-1}).

Fluorescence parameters were also calculated, including regional (e.g., peak A, B, C) peak emission intensities, carbon-normalized peak emission intensities, the fluorescence index (FI), and region-specific maximum emission wavelengths ($\lambda_{em,max}$). [20-22] Region-specific peak intensities were determined using a fixed excitation-emission wavelength pair as well as a peak-picking algorithm by which the excitation-emission pair was allowed to vary within predetermined boundaries until a maximum was found. The corresponding carbon-normalized peak intensities were calculated by dividing the fluorescence intensities by DOC concentration (to give units of RU L mg_C^{-1}). FI is the ratio of intensities at emission wavelengths of 470 nm and 520 nm at a 370 nm excitation wavelength. Table ESI S2 contains additional information regarding calculation of spectroscopic parameters in this study.

The apparent fluorescence quantum yield (Φ_f) was calculated relative to quinine sulfate, a well-established fluorescence standard with a quantum yield of 0.51 in 0.1 N H_2SO_4 based on equation 1:[23]

$$\Phi_{f,DOM} = \Phi_{f,QS} \frac{F_{DOM}}{F_{QS}} \frac{f_{QS}}{f_{DOM}} \frac{n_{DOM}^2(\lambda_{em})}{n_{QS}^2(\lambda_{em})} \quad (1)$$

In this equation, Φ_f is the quantum yield, F is the integrated fluorescence intensity, f is the absorbance factor, λ is the wavelength (either excitation or emission), and n is the refractive

index, with QS representing the values in the quinine sulfate reference standard solution and DOM representing the values in a WEOM sample. Each term above is for a fixed excitation wavelength. An absorbance factor of $1\text{-}10^{-Abs}$ was used. Φ_f describes the likelihood of fluorescence occurring in an excited DOM molecule following absorption of a photon, and this parameter been used as a proxy for DOM physicochemical properties. Additional details on the calculation and application of Φ_f to organic matter analysis can be found elsewhere.[24]

Results and Discussion

Effect of heating on organic carbon release from leached soils

Thermal alteration of mineral and organic soils had a significant effect on the quality of WEOM. Figure 1 presents the percent of WEOC (left panel) and WEON (right panel) for the NED site. WEOC or WEON for each heating temperature (T) were calculated as

$$WEOC_T \text{ or } WEON_T = \frac{DOC_T \text{ or } DON_T \text{ (mg L}^{-1}) \times V_{leachate} \text{ (L)}}{M_{solid\ leached} \text{ (mg)} \times \%C_T \text{ or } \%N_T} \times 100 \quad (2)$$

where DOC and DON are the concentrations of organic carbon and nitrogen, $V_{leachate}$ is the volume used to leach the soil (1 L), $M_{solid\ leached}$ is the mass of soil leached (5 g and 0.2 g for mineral and organic soil, respectively), and %C and %N are the mass percentages of carbon and nitrogen. The numerator represents the mass of organic carbon or nitrogen extracted, and the denominator represents the mass of organic carbon or nitrogen in the soil. The result is the percent of WEOC or WEON.

%C and %N of the soils decreased with increasing heating temperature (Figure S1) as expected due to formation of gaseous products during heating. Interestingly, the N weight percent in mineral soil did not change significantly until 350 ºC. Despite the consistent decrease in %C and %N of the heated soils, the percentage of WEOC and WEON increased

as a result of heating in mineral soil, indicating increased solubility of the organic matter. Maximum WEOC and WEON percentages were observed at 350 ºC and 250 ºC, respectively. Conversely, WEOC and WEON for the organic layer exhibited an approximately five-fold decrease between the CTRL/150 ºC samples and 250 ºC and higher temperature samples. Hogue and Inglett observed that extractable DON peaked around 350 ºC for combustion of herbaceous plant biomass, a similar temperature to that observed in this study for mineral and organic soil, of which plant biomass is one component.[25] Wang et al. observed a peak in WEON and WEOC at a temperature of 250 ºC for pyrogenically heated fir and pine detritus; however, a decrease in the same parameters was observed for heated fir and pine detritus undergoing thermal oxidation. [13] The trends observed by Wang et al. are consistent with our results for *organic* soil, with the difference that WEON and WEOC in our samples did not change significantly until 350 ºC heating (as opposed to 250 ºC heating).

These results indicate that low-moderate temperature heating may increase the solubility of the DOC and DON remaining in soil, despite combustion losses. The increased solubility of organic carbon and nitrogen at low-moderate heating temperatures could be the combined effect of physical and chemical changes in soils that influence WEOM composition. A previous report demonstrated that increasing temperature disrupts soil aggregates due to vaporization of pore water, and exposes physically protected soil organic matter (SOM) to leaching. [26] Our work suggests that, in addition to possible physical processes, changes in SOM chemical structure could also explain increased WEOC and WEON in heated mineral soils.[15] Cawley et al. observed that for soils heated at 225-350 ℃, the WEOM included higher proportions of condensed aromatic structures, such as

black carbon and black nitrogen.[15] These findings are consistent with field studies that have observed post-fire increases in black carbon exports.[27] Condensed aromatic structures present in WEOM mobilized from a wildfire-impacted watershed have the potential to influence water treatment processes and environmental processes involving organic matter.

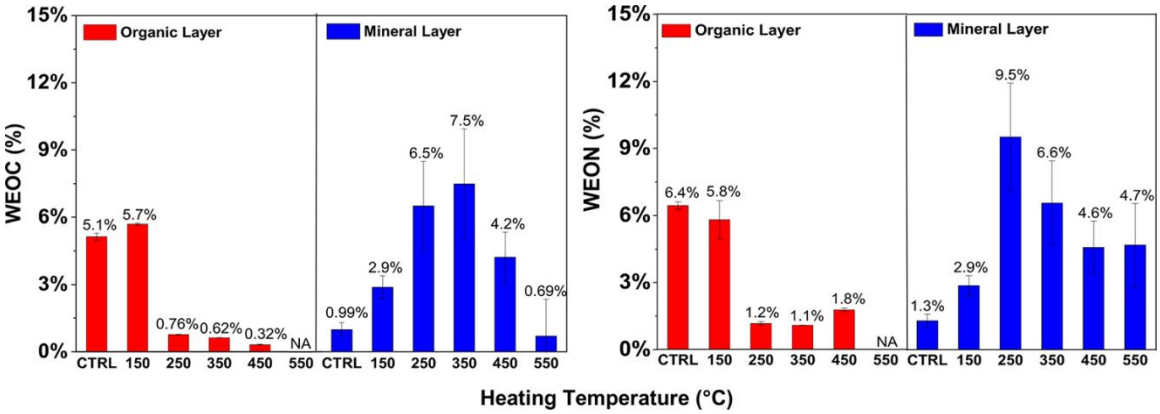

Figure 1. Water extractable organic carbon (WEOC-left) and nitrogen (WEON-right) for both organic and mineral soil horizons from the Nederland site. Mineral and organic soil were leached at 5 and 0.2 g L^{-1}, respectively. WEOC and WEON were calculated according to equation 2. CTRL = control. Reproduced with permission from Hohner et al.[7] Copyright American Chemical Society.

Absorbance and fluorescence spectra of leachates from unheated soil and litter.

Figure 2 presents carbon-normalized absorbance and fluorescence spectra for unheated and thermally altered soil leachates from NED. Identical plots for FLG are shown in ESI Figure S2 and all optical properties are presented in Table 1. Before considering the effect of thermal alteration on WEOM, it is worth comparing the optical properties of WEOM from unheated soil to other types of dissolved organic matter. The molar extinction coefficients for NED mineral and organic soil at 254 nm are ~ 400 and 150 M_C^{-1} cm^{-1} (Figure 2a and 2d), respectively. These extinction coefficients correspond to $SUVA_{254}$ values of 3.3 and 1.3 L mg_C^{-1} m^{-1}. These values are lower than those for soil humic and fulvic acid isolates distributed by the International Humic Substances Society (IHSS); for example, $SUVA_{254}$ values for Pahokee Peat humic and fulvic acid (6.3 and 8.3 L mg_C^{-1} m^{-1},

respectively) are higher. [24] The discrepancy in $SUVA_{254}$ between mineral soil leachates and isolated humic substances is reasonable given the affinity of

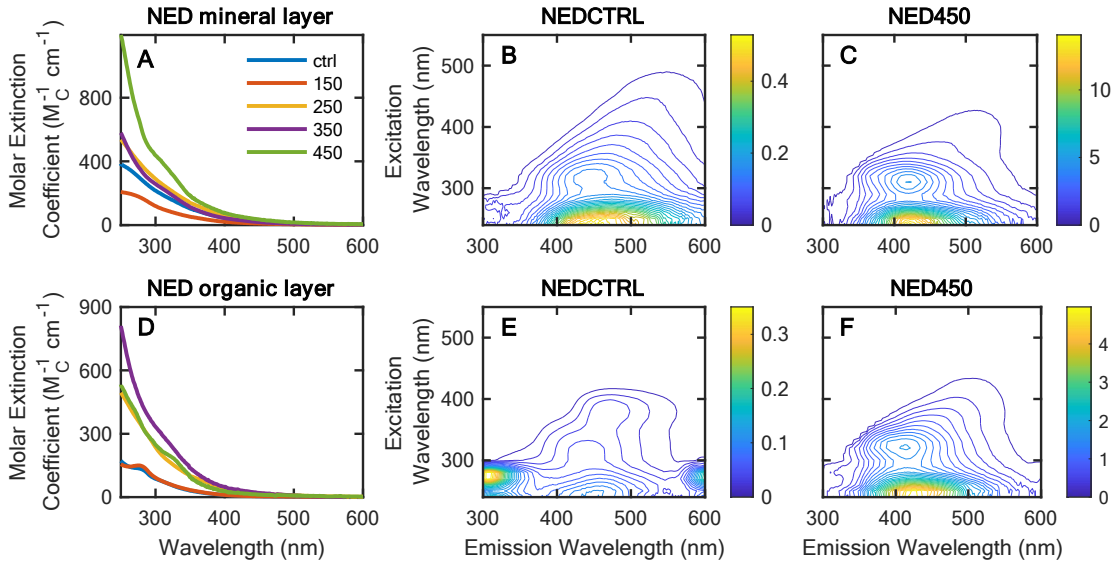

Figure 2. Change in optical properties of water-soluble organic matter from soil (top row) and litter (bottom row) from Nederland site. (A and D) Absorbance spectra normalized to carbon concentration. (B-C and E-F) Fluorescence spectra normalized to carbon concentration (units of RU L mg_C^{-1}).

aromatic moieties for XAD resin used during humic substance isolation[28] compared to the aqueous leaching process for soil extracts, which did not employ any isolation procedures post-filtration. In other words, the leachates for unheated soils do not appear to be composed predominantly of highly aromatic structures. $SUVA_{254}$ values for mineral and organic soil leachates in our study are similar to values from previous studies focused primarily on the organic layer in soils. [13,29-31] When compared to other sources of organic matter, the $SUVA_{254}$ values for soil leachates are more similar to values from filtered whole water samples, including surface water and wastewater-derived effluent organic matter (~ 2 L mg_C^{-1} m^{-1}).[32] The overlap in $SUVA_{254}$ values implies an overall degree of similarity in aromatic carbon content between these different classes of organic matter. Other

absorbance-based optical properties for unheated soil leachates (e.g., *E2/E3*, $S_{300\text{-}600}$) follow the same trends just discussed with regards to $SUVA_{254}$.

Fluorescence EEMs for unheated NED mineral (Figure 2b) and organic soil (Figure 2e) leachates are substantially different in appearance. EEMs for unheated mineral soil leachates are similar to spectra for surface water and humic substance isolates, with the most intense signals being peaks A and C. Isolated *soil* humic substance's fluorescence spectra do not exhibit peak B or T fluorescence, rather significantly red shifted peak A and C emission maxima as well as emission at excitation wavelengths extending far into the red. Conversely, EEMs for unheated organic soil leachates were much more intense in the peak B/T region, which has been attributed to less processed material. [21,22,33] FLG mineral and organic soil leachates (ESI Figure S2) showed similar results. Interestingly, a previous study examining both oxic and anoxic combustion of detritus derived from ponderosa pine and white fir observed peak B/T intensity in leachates of *anoxically heated* samples, but not unheated or oxically heated detritus.[13]

Absorbance and fluorescence spectra of leachates from heated soils.

Thermal alteration of soil resulted in changes to the absorbance and fluorescence spectra of leached material, and these changes were most significant at heating temperatures greater than 150 ºC. Molar extinction coefficients for mineral soil leachates decreased when the material was heated to 150 ºC but were unchanged for the corresponding organic soil samples (Figures 2a and 2d). Leachates for soils heated at 250 ºC and greater exhibited increasing molar extinction coefficients, with maximum values occurring at 450 ºC, approximately three to five times greater than leachates from unheated soil. The maximum $SUVA_{254}$ values observed for these samples were for 450 ºC heated mineral soil (9.3 and

12.6 L mg_C^{-1} m^{-1} for NED and FLG, respectively). Previous studies have observed elevated $SUVA_{254}$ values in both wildfire-impacted whole water samples and laboratory-heated soil leachates;[12-15] however, these previous measurements are below the exceptionally high $SUVA_{254}$ values reported here for 450 ºC heated NED and FLG mineral soil leachates.

These high $SUVA_{254}$ values are outside the range considered normal for surface waters (~1 – 5 L mg_C^{-1} m^{-1}).[19,34,35] Aqueous iron (III) can influence measured $SUVA_{254}$ due to absorption by complexes and oxyhydroxide colloids.[35] However, aqueous iron concentrations for soil leachates were found to be negligible (< 0.05 mg L^{-1}) for all heating temperatures (ESI Table S3). Nitrate can similarly have an impact on absorbance in the UV region of the spectrum at sufficiently high concentrations (ε_{254} ~ 12 M^{-1} cm^{-1}). [36] Although nitrate levels were not characterized for these samples, the highest total nitrogen concentration measured was 5 mg_N/L (ESI Table S4), yielding a maximum possible nitrate concentration of 0.35 mM. For these reasons, it does not seem likely that iron or nitrate significantly contributed to sample absorbance at 254 nm. A possible explanation discussed in more detail below (see ***Mechanistic model to explain results***) is that WEOM in heated soil leachates results in a high fraction of aromatic carbon relative to WEOM from unheated soil.

Although variation was observed in other absorbance-based parameters, such as *E2/E3* or $S_{300\text{-}600}$ (Table 1), there was no consistent trend with heating temperature. Mineral soil from NED was the one exception in that a general increase in *E2/E3* and $S_{300\text{-}600}$ was observed with increasing heating temperature.

Carbon-normalized fluorescence EEMs of heated soil leachates exhibited increases in intensity and changes in spectral shape. Figures 2c and 2f show EEMs for 450 ºC heated

NED mineral and organic soil leachates, respectively (results for FLG soil are shown in ESI Figure S2). EEMs for all samples (both in RU and RU normalized to DOC concentration) at all heating temperatures are shown in ESI Figure S3.

For NED mineral soil, the carbon-normalized intensity of peak A increased more than twenty-fold between the CTRL and 450 ºC heated sample. In addition, the maximum emission wavelength decreased by ~ 30 nm for peak A and ~ 20 nm for peak C for NED mineral and organic soil over this same temperature range. These increases in intensity and shifts in emission maximum were incremental in nature, which can be observed in ESI Figure S3.

The change in fluorescence EEMs in WEOM from organic soil leachates are much more pronounced. An increase in carbon-normalized fluorescence intensity with soil heating temperature is observed for NED organic soil leachate, similar to the mineral soil. Peak B, which is the most intense signal in the unheated organic soil leachate, is completely absent in the 450 ºC leachate. Figure ESI S3 demonstrates that peak B is present in EEMs for the 150 ºC heated organic soil, but not the 250 ºC sample. Similar to heated mineral soil leachates, a decrease in maximum emission wavelength is observed for peak A in heated organic soil leachates (i.e., ~30 nm). However, despite a ~20 nm decrease between the CTRL and 350 ºC heated organic soil, the 450 ºC sample's peak C maximum emission wavelength increased by ~10 nm compared to the 350 ºC leachate.

Table 1. Optical properties for water extractable organic matter from NED and FLG mineral and organic soil leachates. Standard deviations for each measurement are such that the coefficient of variance (standard deviation divided by mean) is less than 5%.

Sample	UV_{254} (cm^{-1})	$SUVA_{254}$ (L mg_C^{-1} m^{-1})	*E2/E3*	*S* (nm^{-1})	S_R	A (RU)	B (RU)	C (RU)	T (RU)	FI	Peak Em 370 (nm)	SpA (RU L mg_C^{-1})	SpB (RU L mg_C^{-1})	SpC (RU L mg_C^{-1})	SpT (RU L mg_C^{-1})	Φ_t 370 nm
NED CTRL mineral soil	0.015	3.1	4.49	0.0153	0.794	0.39	0.05	0.19	0.06	1.23	474	0.5	0.1	0.2	0.1	0.0147
NED 150 mineral soil	0.013	1.7	4.99	0.0167	0.830	0.70	0.12	0.35	0.14	1.25	472	0.2	0	0.1	0.1	0.0133
NED 250 mineral soil	0.029	4.3	4.58	0.0158	0.737	11.32	0.84	6.54	1.56	1.16	474	1.4	0.1	0.7	0.2	0.0286
NED 350 mineral soil	0.083	4.5	6.32	0.0179	0.772	11.72	0.25	5.90	0.91	1.21	448	3.6	0.1	1.6	0.5	0.0827
NED 450 mineral soil	0.108	9.4	8.01	0.0181	1.121	3.74	0.25	1.72	0.41	1.43	448	12.7	0.7	5.0	1.8	0.1080
NED CTRL organic soil	0.025	1.3	7.11	0.0218	0.866	4.18	17.31	2.51	8.06	1.78	466	0.1	0.35	0.1	0.2	0.0247
NED 150 organic soil	0.016	1.2	6.03	0.0204	0.804	4.68	22.65	3.03	10.62	1.77	464	0.1	0.41	0.1	0.3	0.0157
NED 250 organic soil	0.039	4.0	5.79	0.0169	0.886	8.21	0.99	4.95	1.38	1.17	476	1.3	0.18	0.6	0.2	0.0391
NED 350 organic soil	0.032	6.2	7.46	0.0195	0.697	25.77	0.40	13.04	1.78	1.33	448	5.4	0.17	2.4	0.7	0.0318
NED 450 organic soil	0.066	4.2	7.73	0.0216	0.676	3.62	0.33	1.49	0.45	2.09	446	5.1	0.37	1.9	0.8	0.0656
FLG CTRL mineral soil	0.013	2.5	5.08	0.0165	0.773	0.70	0.12	0.32	0.12	1.29	472	0.4	0.1	0.1	0.1	0.0131
FLG 150 mineral soil	0.011	1.9	5.50	0.0168	0.883	1.41	0.63	0.69	0.65	1.32	474	0.2	0.1	0.1	0.1	0.0111
FLG 250 mineral soil	0.041	4.2	5.24	0.0169	0.738	8.31	0.55	4.89	1.04	1.09	476	1.8	0.1	0.9	0.2	0.0406
FLG 350 mineral soil	0.099	7.4	6.53	0.0178	0.788	11.46	0.25	5.99	0.95	1.18	446	6.8	0.2	2.9	0.8	0.0992
FLG 450 mineral soil	0.065	12.6	5.25	0.0128	2.246	1.31	0.55	0.64	0.77	1.72	436	8.4	3.3	3.9	3.6	0.0652
FLG CTRL organic soil	0.018	1.2	7.77	0.0227	1.296	5.70	35.79	3.05	16.22	2.00	466	0.1	0.5	0.1	0.4	0.0183
FLG 150 organic soil	0.014	1.1	6.80	0.0223	0.896	4.81	24.35	3.67	11.84	1.92	462	0.1	0.4	0.1	0.3	0.0136
FLG 250 organic soil	0.027	2.2	6.87	0.0179	0.972	6.28	0.23	3.42	0.49	1.19	474	1.2	0.1	0.6	0.1	0.0273
FLG 350 organic soil	0.066	3.0	9.30	0.0203	0.941	4.84	0.15	2.51	0.41	1.28	458	2.2	0.1	1.0	0.3	0.0660
FLG 450 organic soil	0.108	4.1	7.72	0.0207	0.744	3.99	0.07	2.02	0.14	1.67	456	4.7	0.1	2.0	0.3	0.1082

The results described above are consistent with some aspects of previous reports but disagree with others. Multiple studies have demonstrated an increase in specific absorbance, both at 254 nm, other UV wavelengths, and visible wavelengths,[13,14] for laboratory heated soils and wildfire-impacted soil (white and black ash) leachates, consistent with the results presented in Figure 2, ESI Figure S2, and Table 1. These same studies report increased *E2/E3* and FI in leachates for heated samples, whereas we observed no consistent trend in these values with heating temperature (Table 1).[13,14] Although there were slight differences between studies in sample collection and processing, it is difficult to understand exactly how these differences would result in dissimilar results. Additional work is required to resolve these discrepancies.

Previous studies have focused on the FI of WEOM as an indicator of soil thermal alteration.[12-14,37] A statistically significant increase in FI (1.36 to 1.40, mean of 21 samples) was reported in the Cache la Poudre River after the High Park Fire in Colorado, USA. [12] In addition, leachates of detritus associated with the Rim Fire in California had higher FI values (1.51 and 1.63 for black and white ash, respectively) relative to the control (FI of 1.41). [14] A laboratory study examining the effect of heating temperature and oxygen availability likewise reported increases in FI (by approximately a factor of two) between control samples (FI ~ 1.4) and samples heated at 400 ºC (FI ~2.4). Soil heating has therefore been associated with an increased FI value in the corresponding leachates, which has been used to suggest that DOM molecules in these leachates are smaller and less complex than the corresponding unheated soil leachates. [13,14,37]

FI values measured in our study, however, did not show a consistent increase with heating temperature (Table 1). Based on the blue-shifting fluorescence spectra observed in

ESI Figure S3 and Table 1, we suspected that the first emission wavelength for the FI calculation (470 nm) was no longer centered on the emission peak, which may introduce bias into the FI values and confound interpretation. [22] To assess this question, we calculated the local curvature at an excitation wavelength of 370 nm as described by Korak et al. [22] The specifics of this analysis are described in ESI Text S2 and results are presented in ESI Figures S4 and S5. Briefly, due to blue-shifting maximum emission wavelength, the use of FI may not be appropriate for assessing DOM characteristics such as molecular weight and aromaticity *for heated mineral and organic soil WEOM* because of the difference in peak emission maxima and 470 nm (I_1 in the FI calculation). Nevertheless, the conclusions drawn from these previous studies are likely still correct (see ***Mechanistic model to explain results***).

Apparent fluorescence quantum yields.

Apparent fluorescence quantum yields (Φ_f) were measured for unheated and thermally altered soil leachates. Based on the large increases in fluorescence intensity observed with increasing soil heating temperature in Figure 2, we hypothesized that Φ_f values would be larger for thermally altered soil leachates. Φ_f represents the probability of absorbed light being emitted as fluorescence compared to other pathways, which include non-radiative (internal conversion, intersystem crossing) and radiative processes (phosphorescence). Φ_f values for DOM have been measured in previous studies and range from < 0.005 to ~ 0.03.[24,32,38-41] Because of this approximately order of magnitude in variability, Φ_f has greater potential for identifying the presence of thermally altered water extractable organic matter than other optical properties, which do not exhibit as large of a range as Φ_f.

Figure 3 shows Φ_f values as a function of excitation wavelength for unheated and thermally altered NED mineral (Figure 3a) and organic (Figure 3b) soil layers compared to analogous values for selected DOM isolates and whole water samples (Figure 3c). Data from FLG is shown in ESI Figure S6. Φ_f values for unheated soil leachates were ~0.01-0.03 at an excitation wavelength of 370 nm. Larger Φ_f values were observed at excitation wavelengths around 400 nm. These values are generally higher than humic substance isolates (typically < 0.01), especially soil humic substances (e.g., ESHA in Figure 3c), but are similar to values for EfOM. [32]

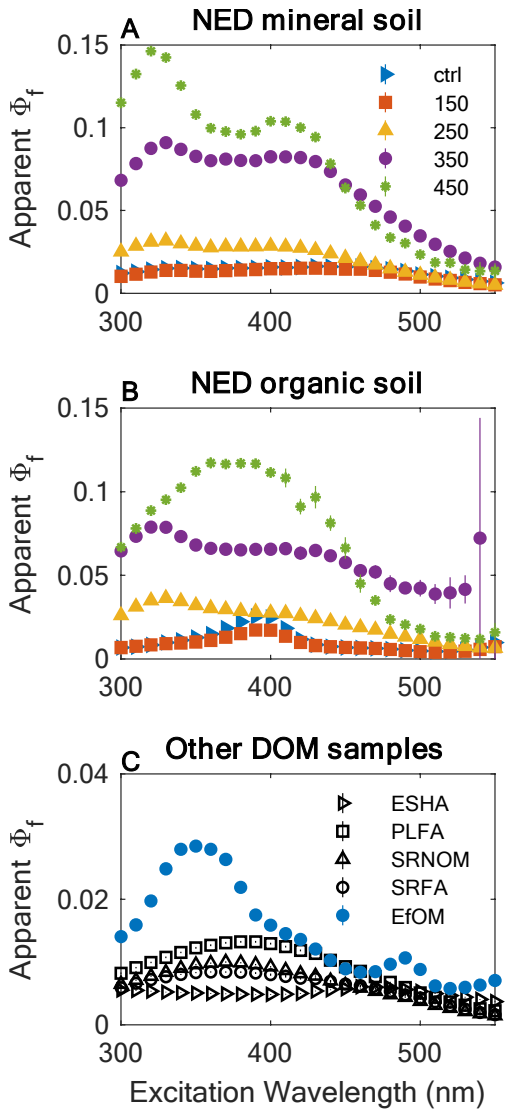

Figure 3. Apparent fluorescence quantum yields (Φ_f) for (A) Nederland mineral soil leachates, (B) Nederland organic soil leachates, and (C) select DOM samples. For 3a and 3b, colors represent different soil heating temperatures (in ºC). For Figure 3c, different symbols represent various organic matter types: ESHA (Elliot Soil humic acid I), PLFA (Pony Lake fulvic acid), Suwannee River Natural Organic Matter (SRNOM II), Suwannee River fulvic acid (SRFA I), and EfOM (effluent organic matter). Error bars represent the standard deviation from duplicate measurements. If not visible, then the error bars are smaller than the symbols.

An increase in Φ_f was observed for WEOM from heated soil (Figures 3a and 3b, ESI Figures S6a and S6b). As with specific absorbance and fluorescence values, Φ_f remained relatively unchanged between unheated and 150 ºC heated soil leachates. However,

leachates derived from material heated at 250 ºC or higher exhibited significant increases in Φ_f, with values up to ~0.10 recorded for 450 ºC heated samples at an excitation wavelength of 350 nm. The Φ_f values of ~0.10 reported here are approximately an order magnitude greater than the typical range for DOM and approaches values more often observed for small aromatic compounds. [42] As detailed previously, excitation wavelengths < 350 nm for the Fluoromax-4 instrument are subject to instrumental biases that make Φ_f slightly inflated.[24]

Φ_f can also be thought of as the rate of fluorescence relative to the total inactivation rate of the singlet excited state. The increasing Φ_f with increasing soil heating temperature therefore implies that DOM in these samples either i) has a faster rate of fluorescence than other types of DOM, or ii) has slower rates of non-radiative decay (e.g., internal conversion). Although we cannot rule out the first possibility, we expect scenario ii) to be more likely based on the decrease in maximum emission wavelength with increased heating temperature (ESI Figure S3). A blue shift in maximum emission wavelength indicates that fluorescence is occurring from a higher energy first excited singlet state. According to the energy gap law, the rate of radiationless transition is inversely proportional to the energy between the ground and first excited singlet state (rate ~ $e^{-\Delta E}$), which in turn increases with decreasing maximum emission wavelength (shorter wavelength, higher energy). [43,44] We therefore hypothesize that the increase in Φ_f is due to a decrease in the radiationless transition rate. This link between maximum emission wavelength and Φ_f has also been observed recently for DOM undergoing ozonation. [45]

Overall, these results are significant in that they are the highest reported Φ_f values for DOM by more than a factor of two.[24,32,38-41] The implications of this result for assessing the presence of pyrogenic WEOM are discussed below.

Relationship between optical properties and heating temperature.

There was largely no statistically significant difference between optical properties obtained for WEOM from soils heated at 100 ºC and 150 ºC (one-tailed t-test, ESI Table S5). Conversely, most intrinsic optical properties for WEOM exhibited statistically significant differences between the CTRL and soils heated to 250 ºC and higher (ESI Table S5). It is interesting that there appears to be some temperature threshold (between 150 and 250 ºC) required to induce physicochemical modifications in soils that result in changes to WEOM optical properties.

Linear regression analysis was used to quantitatively explore relationships between WEOM optical properties and heating temperature. Because WEOM from control samples dried at 100 ºC was no different than WEOM from soils heated at 150 ºC, the control was not included in the regression analysis. Various optical properties measurements were chosen as the dependent variables, whereas heating temperature (in ºC) was chosen as the independent variable.

The optical properties listed in Table 2 can be separated into extrinsic and intrinsic values. Concentration based parameters such as absorbance and fluorescence intensity are extrinsic, depending on both the quality and quantity of organic matter, while physicochemical properties such as carbon-normalized values, Φ_f, and slope ratios are intrinsic, depending solely on the quality of organic matter. The main extrinsic variables that correlated well with heating temperature were the absorbances at 254 nm and 280 nm.

As shown in Figure 2 and explained above, molar extinction coefficients increased substantially between CTRL and 450 ºC heated soil leachates, and so the decrease in absorbance at 254 and 280 nm can be attributed to decreases in DOC concentration in the leachates (Table S4). All other variables that showed significant correlations with heating temperature were intrinsic parameters based on either absorbance ($SUVA_{254}$) or fluorescence spectra (Φ_f, specific A, specific C, peak C emission maximum, peak emission maximum at 310 nm). Clearly, changes in intrinsic optical properties correlate well to soil heating temperature, which reflects the changes in WEOM physicochemical properties such as molecular weight and aromaticity. From a practical perspective, these results highlight the possibility that each of these optical properties could be used for assessing the contribution of pyrogenic WEOM in wildfire-impacted watersheds. Future studies could assess this application further via an in-stream monitoring approach in which DOM optical properties are compared to background DOM prior to wildfire.

Extension to soil from additional geographic locations

The effect of soil heating on WEOM for three additional locations (10 sites total) was used to assess the generality of our results. Mineral and organic soil layers were collected from three sites (labeled WM) within the Clear Creek watershed (Colorado, USA), three sites (labeled DW) near Gross Reservoir (Colorado, USA) and four sites (labeled NY) in the Catskill Mountains (New York, USA). Additional sample information is provided in ESI Table S1. Mineral and organic soils were collected and processed separately, but then mixed together to form a composite prior to leaching. Composite samples were heated as described previously, but at 225 ºC. Further, these samples were leached in dechlorinated, low-carbon tap water instead of ultra-pure water. Additional information including site

descriptions, soil sampling protocols, processing, and leaching methods are described elsewhere. [46]

Optical properties for composite samples are shown in ESI Table S6 and ESI Figures S7 and S8. ESI Figure S7 shows box plots for selected optical parameters in which all unheated and 225 ºC heated samples are pooled together. A significant increase was observed in the *E2/E3* ratio (p = 0.00417, students one-tailed t test), S_R ($p < 1 \times 10^{-6}$, students one-tailed t test), and Φ_f (p = 0.00156, students one-tailed t test) for heated samples compared to unheated. Conversely, *E2/E3* and $S_{300\text{-}600}$ were not significantly different between unheated and 250 ºC heated soil leachates for NED and FLG. Φ_f of WEOM was higher for heated soils in all cases (ESI Figures S6, S7 and S8).

To assess the adequacy of the correlations shown in Table 2, Φ_f and absorbance at 254 nm for heated samples were used to calculate the apparent heating temperature (known to be 225 ºC) for the composite samples. Importantly, these correlations were based on independently heated and leached organic and mineral soils (see Materials and Methods, *Soil collection and processing*) whereas the test samples were composites. Average heating temperatures of 250 ± 50 ºC and 470 ± 10 ºC were calculated using the regression equations for Φ_f and absorbance at 254 nm, respectively.

Heating temperatures predicted using Φ_f agreed well with the experimental value of 225 ºC (range of 170 to 330 ºC). Heating temperatures calculated using absorbance at 254 nm as a predictor significantly overestimated the actual value. This result suggests that intrinsic optical properties, which are normalized for WEOM quantity, may be more suitable for predicting both the presence and severity of wildfire-impacted WEOM in a given surface water.

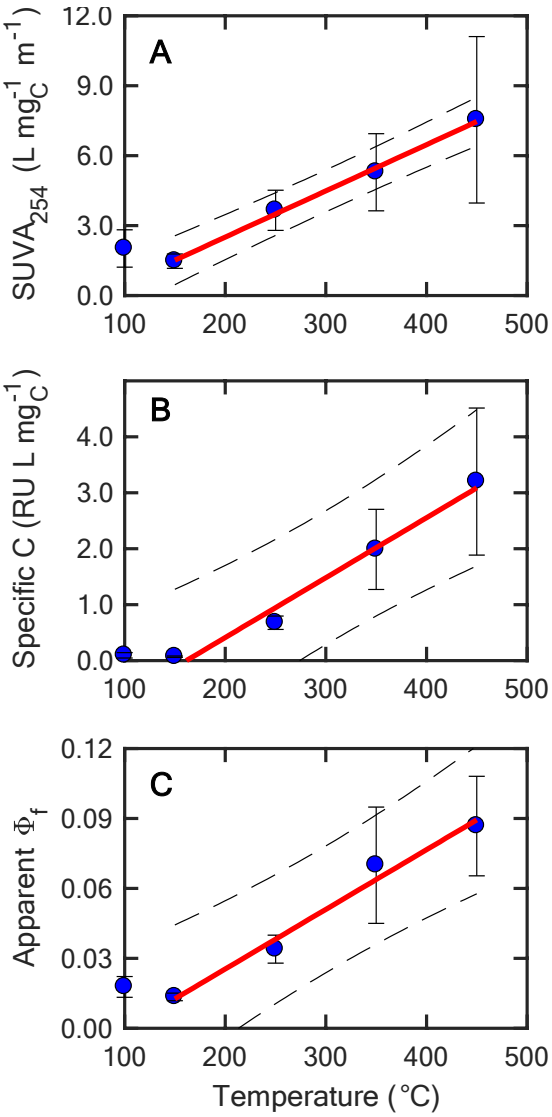

Figure 4. Relationships between optical properties and temperature for water extractable organic matter from thermally altered soils from Nederland and Flagstaff sites. Data points represent the mean of soil leachates from both sites and different soil horizons (mineral and organic) at the specified heating temperature (4 samples for each data point). Control samples were plotted at 100 ºC (the temperature all soils were dried at) and are not included in the regression. Error bars represent the standard deviation from the 4 samples. Dashed lines represent 95% prediction intervals. Equations for all regressions are provided in Table 2.

Table 2. Regression parameters for optical properties and heating temperature for water soluble organic carbon from thermally altered soils from Nederland and Flagstaff sites. Slope and intercept *p* represent the probability that the reported slope and intercept values are no different from zero (at a 95% confidence level).

Dependent variable	Extrinsic/ Intrinsic	Regression equation	Regression diagnostics		
			Slope p	Intercept p	R^2
$SUVA_{254}$	Intrinsic	y = 0.0198x –1.46	0.002	0.032	0.996
Apparent Φ_f	Intrinsic	y = 0.000256x	0.010	0.086	0.981
Specific C	Intrinsic	y = 0.0107x – 1.73	0.011	0.040	0.979
Abs_{254}	Extrinsic	y = -0.00122x + 0.612	0.011	0.004	0.978
$SUVA_{280}$	Intrinsic	y = 0.0111x	0.014	0.477	0.973
Specific A	Intrinsic	y = 0.0258x	0.016	0.056	0.968
Abs_{280}	Extrinsic	y = -0.00126x + 0.575	0.017	0.008	0.967
Peak C emission maximum	Intrinsic	y = -0.0635x + 442	0.021	< 0.001	0.959
Emission maximum at 310 nm	Intrinsic	y = -0.0865x + 447	0.022	< 0.001	0.956

Mechanistic model to explain results.

Optical property data for our heat altered soil leachates provide an indirect assessment of DOM physicochemical properties. We therefore sought to use a more direct method to assess changes in WEOM due to soil heating, namely size exclusion chromatography (SEC). A subset of the samples described in the ***Extension to soil from additional geographic locations*** section (also see ESI Table S1) were characterized by SEC as part of a separate study (ESI Figure S9). [47] The optical data corresponding to the average across all samples (WM, DW and NY, 10 total), for which these SEC data are a subset of, are shown in ESI Figure S7. SEC chromatograms for these heated soil extracts demonstrate a consistent shift towards longer retention times (lower molecular weight). While we unfortunately do not have SEC characterization on all samples from the NED and FLG sites, results shown in Figure S9 are corroborated by previous studies demonstrating shifts to lower molecular weight in WEOM from heated soil. [15]

Overall, our results suggest that WEOM derived from thermally altered soil leachates is lower in molecular weight and more aromatic than leachates derived from unheated soils.

$SUVA_{254}$, a parameter positively correlated with aromaticity, increased as heating temperature was raised, indicating that the WEOM is becoming more aromatic. This is consistent with previous reports that show an increased amount of black nitrogen and black carbon in thermally altered WEOM. [15,27,37,48] Conversely, other parameters traditionally used to assess DOM molecular weight (*E2/E3*, $S_{300\text{-}600}$, and S_R) do not provide as clear of a picture regarding changes in WEOM molecular weight and aromaticity from heated soil leachates.

Although the conclusions made above are consistent with the reported optical data, a natural progression of this work would be to apply additional, molecular level, characterization methods (e.g., ultra high resolution mass spectrometry, 2-D nuclear magnetic resonance) to these samples. Efforts in this area are currently underway as part of a forthcoming study describing the NED and FLG samples discussed herein, as well as additional sample sites.

A significant finding from this research is the decoupling of $SUVA_{254}$ from organic matter molecular weight. These two parameters are usually positively correlated, [32,49] but in our study are inversely correlated, which we attribute to the formation of more aromatic, lower molecular weight molecules.

Environmental Implications

Predicting environmental responses to wildfires in forested watersheds is a complex task. The effect of wildfire on water quality, including not just WEOM quantity but also quality, can significantly impact natural and engineered processes. This study characterized the optical properties of WEOM from laboratory heated soil leachates in order to better understand the physicochemical changes occurring in WEOM as a result of soil heating,

with the intention that these optical properties can be used as surrogates for tracking the contribution and fate of pyrogenic organic matter post-fire.

We observed systematic changes in WEOM absorbance and fluorescence spectra in WEOM from laboratory heated soil. Spectral shape, intensity, and changes in various optical metrics support the hypothesis that heating of mineral and organic soil results in a higher proportion of lower molecular weight, more aromatic molecules in WEOM.

From a monitoring perspective, future work is needed to verify which optical properties best describe WEOM impacted by wildfire, but our results suggest that intrinsic parameters are best, including $SUVA_{254}$, Φ_f, and peak emission maximum at various excitation wavelengths. While the three above optical parameters all showed excellent correlations with heating temperature, their use in online or remote monitoring may be hampered as current optical sensor technology does not routinely utilize full emission scans, nor are in-stream DOC sensors used. However, high frequency (e.g., weekly) and episodic (e.g., rainfall) sample collection and offline analysis may still provide insight into WEOM characteristics post-fire, especially over longer time scales for which post-fire impacts are currently less understood. In addition, new sensor technology may allow for full spectral characterization of WEOM in the coming years, making use of these intrinsic optical properties possible.

Acknowledgments

The authors acknowledge support from the US Environmental Protection Agency (Grant # R835865) and the National Science Foundation (Award #1512705). The authors also acknowledge Yun Yu, Ariel Retuta, and Jenna Crouch for sample collection/processing and collecting fluorescence data, respectively. We thank Prof. Julie Korak providing a portion of the Matlab code used to analyze the results.

References

(1) Jolly, W. M.; Cochrane, M. A.; Freeborn, P. H.; Holden, Z. A.; Brown, T. J.; Williamson, G. J.; Bowman, D. M. J. S. Climate-induced variations in global wildfire danger from 1979 to 2013. *Nature Communications* **2015**, *6* (1), 7537.

(2) Liu, Y.; Stanturf, J.; Goodrick, S. Trends in global wildfire potential in a changing climate. *Forest Ecology and Management* **2010**, *259* (4), 685–697.

(3) Hurteau, M. D.; Westerling, A. L.; Wiedinmyer, C.; Bryant, B. P. Projected effects of climate and development on California wildfire emissions through 2100. *Environmental Science & Technology* **2014**, *48*, 2298–2304.

(4) Radeloff, V. C.; Helmers, D. P.; Kramer, H. A.; Mockrin, M. H.; Alexandre, P. M.; Bar-Massada, A.; Butsic, V.; Hawbaker, T. J.; Martinuzzi, S.; Syphard, A. D.; et al. Rapid growth of the US wildland-urban interface raises wildfire risk. *Proceedings of the National Academy of Sciences* **2018**, *115* (13), 3314–3319.

(5) Bladon, K. D.; Emelko, M. B.; Silins, U.; Stone, M. Wildfire and the Future of Water Supply. *Environmental Science & Technology* **2014**, *48* (16), 8936–8943.

(6) Smith, H. G.; Sheridan, G. J.; Lane, P. N. J.; Nyman, P.; Haydon, S. Wildfire effects on water quality in forest catchments: A review with implications for water supply. *Journal of Hydrology* **2011**, *396* (1-2), 170–192.

(7) Hohner, A. K.; Rhoades, C. C.; Wilkerson, P.; Rosario-Ortiz, F. L. Wildfires alter forest watersheds and threaten drinking water quality. *Accounts of Chemical Research* **2019**, *52* (5), 1234–1244.

(8) Rhoades, C. C.; Entwistle, D.; Butler, D. The influence of wildfire extent and severity on streamwater chemistry, sediment and temperature following the Hayman Fire, Colorado. *International Journal of Wildland Fire* **2011**, *20* (3), 430.
(9) Neary, D. G.; Ryan, K. C.; DeBano, L. F. Wildland fire in ecosystems: effects of fire on soils and water. *Gen. Tech. Rep. RMRS-GTR-42-vol* **2005**, *4*, 250.
(10) Moody, J. A.; Shakesby, R. A.; Robichaud, P. R.; Cannon, S. H.; Martin, D. A. Current research issues related to post-wildfire runoff and erosion processes. *Earth Science Reviews* **2013**, *122*, 10–37.
(11) Murphy, S. F.; Writer, J. H.; McCleskey, R. B.; Martin, D. A. The role of precipitation type, intensity, and spatial distribution in source water quality after wildfire. *Environmental Research Letters* **2015**, *10* (8), 1–13.
(12) Hohner, A. K.; Cawley, K.; Oropeza, J.; Summers, R. S.; Rosario-Ortiz, F. L. Drinking water treatment response following a Colorado wildfire. *Water Research* **2016**, *105* (C), 187–198.
(13) Wang, J.-J.; Dahlgren, R. A.; Chow, A. T. Controlled burning of forest detritus altering spectroscopic characteristics and chlorine reactivity of dissolved organic matter: Effects of Temperature and oxygen availability. *Environmental Science & Technology* **2015**, *49* (24), 14019–14027.
(14) Wang, J.-J.; Dahlgren, R. A.; Erşan, M. S.; Karanfil, T.; Chow, A. T. Wildfire altering terrestrial precursors of disinfection byproducts in forest detritus. *Environmental Science & Technology* **2015**, *49* (10), 5921–5929.
(15) Cawley, K. M.; Hohner, A. K.; Podgorski, D. C.; Cooper, W. T.; Korak, J. A.; Rosario-Ortiz, F. L. Molecular and spectroscopic characterization of water extractable organic matter from thermally altered soils reveal Insight into disinfection byproduct precursors. *Environmental Science & Technology* **2017**, *51* (2), 771–779.
(16) Peuravuori, J.; Pihlaja, K. Molecular size distribution and spectroscopic properties of aquatic humic substances. *Analytica Chimica Acta* **1997**, *337*, 133–149.
(17) Twardowski, M. S.; Boss, E.; Sullivan, J. M.; Donaghay, P. L. Modeling the spectral shape of absorption by chromophoric dissolved organic matter. *Marine Chemistry* **2004**, *89* (1-4), 69–88.
(18) Helms, J. R.; Stubbins, A.; Ritchie, J. D.; Minor, E. C.; Kieber, D. J.; Mopper, K. Absorption spectral slopes and slope ratios as indicators of molecular weight, source, and photobleaching of chromophoric

dissolved organic matter. *Limnology and Oceanography* **2008**, *53* (3), 955–969.

(19) Weishaar, J. L.; Aiken, G. R.; Bergamaschi, B. A.; Fram, M. S.; Fujii, R.; Mopper, K. Evaluation of specific ultraviolet absorbance as an indicator of the chemical composition and reactivity of dissolved organic carbon. *Environmental Science & Technology* **2003**, *37* (20), 4702–4708.

(20) Coble, P. G. Characterization of marine and terrestrial DOM in seawater using excitation emission matrix spectroscopy. *Marine Chemistry* **1996**, *51* (4), 325–346.

(21) McKnight, D. M.; Boyer, E. W.; Westerhoff, P. K.; Doran, P. T.; Kulbe, T.; Andersen, D. T. Spectrofluorometric characterization of dissolved organic matter for indication of precursor organic material and aromaticity. *Limnology and Oceanography* **2001**, *46* (1), 38–48.

(22) Korak, J. A.; Dotson, A. D.; Summers, R. S.; Rosario-Ortiz, F. L. Critical analysis of commonly used fluorescence metrics to characterize dissolved organic matter. *Water Research* **2014**, *49*, 327–338.

(23) Velapoldi, R. A.; Mieleaz, K. D. *Standard Reference Materials: A fluorescence standard reference material*; National Institute of Standards and Technology: Gaithersburg, MD, 1980.

(24) McKay, G.; Korak, J. A.; Erickson, P. R.; Latch, D. E.; McNeill, K.; Rosario-Ortiz, F. L. The case against charge transfer interactions in dissolved organic matter photophysics. *Environmental Science & Technology* **2018**, *52* (2), 406–414.

(25) Hogue, B. A.; Inglett, P. W. Nutrient release from combustion residues of two contrasting herbaceous vegetation types. *Science of The Total Environment* **2012**, *431*, 9–19.

(26) Jian, M.; Berli, M.; Ghezzehei, T. A. Soil structural degradation during low-severity burns. *Geophys. Res. Lett.* **2018**, *45* (11), 5553–5561.

(27) Wagner, S.; Cawley, K. M.; Rosario-Ortiz, F. L.; Jaffé, R. In-stream sources and links between particulate and dissolved black carbon following a wildfire. *Biogeochemistry* **2015**, *124*, 145–161.

(28) Aiken, G. R.; McKnight, D. M.; Thorn, K. A.; Thurman, E. M. Isolation of hydrophilic organic acids from water using nonionic macroporous resins. *Organic Geochemistry* **1992**, *18* (4), 567–573.

(29) Beggs, K. M. H.; Summers, R. S. Character and chlorine reactivity of dissolved organic matter from a mountain pine beetle impacted

watershed. *Environmental Science & Technology* **2011**, *45* (13), 5717–5724.

(30) Pellerin, B. A.; Hernes, P. J.; Saraceno, J.; Spencer, R. G. M.; Bergamaschi, B. A. Microbial degradation of plant leachate alters lignin phenols and trihalomethane precursors. *Journal of Environment Quality* **2010**, *39* (3), 946–949.

(31) Hansen, A. M.; Kraus, T. E. C.; Pellerin, B. A.; Fleck, J. A.; Downing, B. D.; Bergamaschi, B. A. Optical properties of dissolved organic matter (DOM): Effects of biological and photolytic degradation. *Limnol. Oceanogr.* **2016**, *61* (3), 1015–1032.

(32) Mostafa, S.; Korak, J. A.; Shimabuku, K.; Glover, C. M.; Rosario-Ortiz, F. L. Relation between optical properties and Formation of reactive intermediates from different size fractions of organic matter. In *Advances in the Physicochemical Characterization of Dissolved Organic Matter: Impact on Natural and Engineered Systems*; ACS Symposium Series; American Chemical Society: Washington, DC, 2014; Vol. 1160, pp 159–179.

(33) Aiken, G. *Fluorescence and Dissolved Organic Matter*; Coble, P., Lead, J., Baker, A., Reynolds, D. M., Spencer, R. G. M., Eds.; Cambridge University Press: Cambridge, 2014; pp 35–74.

(34) Spencer, R. G. M.; Butler, K. D.; Aiken, G. R. Dissolved organic carbon and chromophoric dissolved organic matter properties of rivers in the USA. *J. Geophys. Res.* **2012**, *117* (G3), G03001.

(35) Poulin, B. A.; Ryan, J. N.; Aiken, G. R. Effects of iron on optical properties of dissolved organic matter. *Environmental Science & Technology* **2014**, *48* (17), 10098–10106.

(36) Mack, J.; Bolton, J. R. Photochemistry of nitrite and nitrate in aqueous solution: a review. *Journal of Photochemistry and Photobiology* **1999**, *128* (1), 1–13.

(37) Cawley, K. M.; Hohner, A. K.; McKee, G. A.; Borch, T.; Omur-Ozbek, P.; Oropeza, J.; Rosario-Ortiz, F. L. Characterization and spatial distribution of particulate and soluble carbon and nitrogen from wildfire-impacted sediments. *J Soils Sediments* **2018**, 1–13.

(38) Green, S. A.; Blough, N. V. Optical absorption and fluorescence properties of chromophoric dissolved organic matter in natural waters. *Limnol. Oceanogr.* **1994**, *39* (8), 1903–1916.

(39) Del Vecchio, R.; Blough, N. V. On the origin of the optical properties of humic substances. *Environmental Science & Technology* **2004**, *38* (14), 3885–3891.

(40) Boyle, E. S.; Guerriero, N.; Thiallet, A.; Vecchio, R. D.; Blough, N. V. Optical properties of humic substances and CDOM: Relation to structure. *Environmental Science & Technology* **2009**, *43* (7), 2262–2268.

(41) McKay, G.; Couch, K. D.; Mezyk, S. P.; Rosario-Ortiz, F. L. Investigation of the coupled effects of molecular weight and charge-transfer interactions on the optical and photochemical properties of dissolved organic matter. *Environmental Science & Technology* **2016**, *50* (15), 8093–8102.

(42) Lakowicz, J. R. *Principles of Fluorescence Spectroscopy*, Third. Springer, New York, 1999.

(43) Turro, N. J.; Ramamurthy, V.; Scaiano, J. C. *Modern Molecular Photochemistry of Organic Molecules*; University Science Books: Sausalito, California, 2012.

(44) Klán, P.; Wirz, J. *Photochemistry of Organci Compounds*; Wiley, 2009.

(45) Leresche, F.; McKay, G.; Kurtz, T.; Gunten, von, U.; Canonica, S.; Rosario-Ortiz, F. L. Effects of ozone on the photochemical and photophysical properties of dissolved organic matter. *Environmental Science & Technology* **2019**, *53* (10), 5622–5632.

(46) Hohner, A. K.; Webster, J.; Cawley, K. M.; Rosario-Ortiz, F. L.; Becker, W. C. *Wildfire impacts on drinking water treatment process performance: Development of evaluation protocols and management practices*; Denver, CO, 2018; pp 1–122.

(47) Hohner, A. K.; Summers, R. S.; Rosario-Ortiz, F. L. Laboratory simulation of postfire effects on conventional drinking water treatment and disinfection byproduct formation. *AWWA Water Science* **2019**, e1115.

(48) Jaffé, R.; Ding, Y.; Niggemann, J.; Vahatalo, A. V.; Stubbins, A.; Spencer, R. G. M.; Campbell, J.; Dittmar, T. Global charcoal mobilization from soils via dissolution and riverine transport to the oceans. *Science* **2013**, *340* (6130), 345–347.

(49) Maizel, A. C.; Remucal, C. K. Molecular Composition and Photochemical Reactivity of Size-Fractionated Dissolved Organic Matter. *Environmental Science & Technology* **2017**, *51* (4), 2113–2123.